Echo FT-EPR Study of the Photochemical Reduction and Oxidation Reactions of 2,5-Di-*t*-butyl-1,4-benzoquinone and 2,5-Di-*t*-butylhydroquinone by Xanthene Dyes

Akio Katsuki, Kimio Akiyama, and Shozo Tero-Kubota*

Institute for Chemical Reaction Science, Tohoku University, Katahira 2-1-1, Aobaku, Sendai 980

(Received May 26, 1995)

Electron spin polarization has been studied in order to clarify the character of the short-lived radical-pair (RP) intermediates generated from the photosensitized reduction of 2,5-di-*t*-butyl-1,4-benzoquinone and the oxidation of 2,5-di-*t*-butylhydroquinone by xanthene dyes using FT-EPR spectroscopy. Unusual absorptive electron spin polarization and heavy atom effects were observed in a former photoreduction system, indicating the production of contact RP as the reaction intermediate. Absorptive polarization is created by sublevel selective back electron transfer in the triplet contact RP due to the spin-orbit coupling interaction. On the other hand, it has also been shown that for the photooxidation system a pure RP mechanism is operative to create spin polarization, suggesting the generation of a solvent separated RP as an intermediate. The reaction rate constants for electron transfer and hydrogen abstraction reactions were also determined by analyses of the time profile of the chemically induced electron spin polarization spectra.

In our previous paper[1] we proposed a new electron spin polarization mechanism, spin-orbit coupling (SOC) induced electron spin polarization. Chemically induced electron spin polarization (CIDEP) with an unusual net absorptive (A) CIDEP spectra were measured for several quinone anion radicals generated from photoinduced electron transfer reactions between xanthene dyes and *p*-quinones. Since the SOC interaction causes simultaneous changes in the orbital angular and spin operators, sublevel selective back electron transfer from the triplet contact radical pair (RP) to the ground state is induced, leading to a net A spin polarization.

It has been reported that a direct SOC interaction is operative over the short distance of the pair radicals.[2—11] Steiner et al.[6,7] have shown that heavy atom substituents significantly enhance the intersystem crossing (ISC) process of an intermediate triplet exciplex with a radical-pair-like electronic structure produced from the photoinduced electron transfer reactions. They proposed a sublevel selective depopulation of the triplet exciplex, based on magnetic field effects on the decay kinetics and yield of the radicals. Kikuchi et al.[10,11] have reported that the radical yield from singlet contact RP increases with increasing the heavy atoms.

In the present work we studied the CIDEP spectra generated from the photochemical reduction of 2,5-di-*t*-butyl-1,4-benzoquinone (tBu$_2$BQ) and the oxidation of 2,5-di-*t*-butylhydroquinone (tBu$_2$BQH$_2$) by xanthene dyes. The electron spin polarization mechanism and RP intermediates generated in the reaction process are discussed. The reaction rate constants for the electron transfer and hydrogen abstraction reactions were also determined by analyses of the time profiles of the CIDEP spectra observed with the echo FT-EPR method.

Experimental

FT-EPR measurements were carried out using an X-band pulsed EPR spectrometer (Bruker ESP-380E). The resonator used was a dielectric cavity with a low Q value of about 100. To eliminate the dead-time problem in free induction decay (FID) measurements, the electron spin echo signals generated from a two-pulse ($\pi/2$–τ–π, where the width of the $\pi/2$-pulse was 8 ns and τ=88 ns) sequence were detected. The unwanted FID signals were suppressed by an 8-step phase cycling. For phase correction, the non-polarized spectra observed with $\tau_d > 10$ μs (where τ_d is the delay time between the laser and microwave pulses) were used as a reference. A Nd–YAG laser (Quanta-Ray GCR-14S, 532 nm, pulse width of 6 ns, 10 Hz) was used as the light source. The present FT-EPR system has the time resolution of ca. 10 ns.

The purification of tBu$_2$BQ was carefully carried out by vacuum sublimation. tBu$_2$BQH$_2$ and eosin Y (EY) were recrystallized from benzene and ethanol, respectively. Erythrosin B (ER) and 1-propanol were used without purification. All of the samples and solvents were purchased from Nacalai Chemical Co. The sample solutions were deoxygenated by argon gas bubbling and flowed into a quartz cell within an EPR resonator. The measurements were performed on a 1-propanol solution with the following concentrations: 1×10^{-3} mol dm^{-3} tBu$_2$BQ–1×10^{-4} mol dm^{-3} xanthene dye and 3×10^{-3} mol dm^{-3} tBu$_2$BQH$_2$–1×10^{-4} mol dm^{-3} xanthene dye, respectively. Under the present

experimental conditions, electron transfer mainly occurred from the excited triplet (T_1) states of xanthene dyes.[12] All of the measurements were carried out at room temperature.

Results and Discussion

Figure 1 shows the echo FT-EPR spectra generated from the photosensitized reduction of tBu$_2$BQ with EY and ER in 1-propanol at room temperature. The EPR spectra consist of simple triplet hyperfine (hf) lines with $a^H=0.22$ mT and $g=2.0044$. These values agree with those of the corresponding quinone anion radical, tBu$_2$BQ$^-$, reported previously.[13] The counter radicals of the EY and ER radicals were not observed because of the short relaxation time. The results clearly indicate that the time profile of the spin polarization depends on the sensitizer used. In the case of the EY–tBu$_2$BQ system, the net emissive CIDEP spectra were observed during the early time regime; the delay time (τ_d) between the laser and first microwave pulses was $\leqq$60 ns. The net E polarization is attributed to the normal triplet mechanism (TM), because the upper sublevels of the lowest excited triplet (T_1) state are preferentially populated during the ISC process in EY.[14] A weak dispersive spectrum was obtained at $\tau_d \approx 80$ ns, indicating the presence of a spin-correlated radical pair (SCRP).[1,15] Subsequently, enhanced absorption signals appeared. The behavior is very similar to that for the photoreduction of duroquinone by EY.[1] The unusual A signals are due to the SOC-induced spin polarization (discussed later). In contrast to the EY–tBu$_2$BQ system, no E-polarized signal was observed in the ER–tBu$_2$BQ system. This is probably due to the fast electron spin relaxation time in the T_1 state of ER because of the heavy atom effects.

The time profiles of the echo FT-EPR signals of the central hf line for tBu$_2$BQ$^{-\bullet}$ are depicted in Fig. 2. Because the electron spin relaxation times of the T_1 state

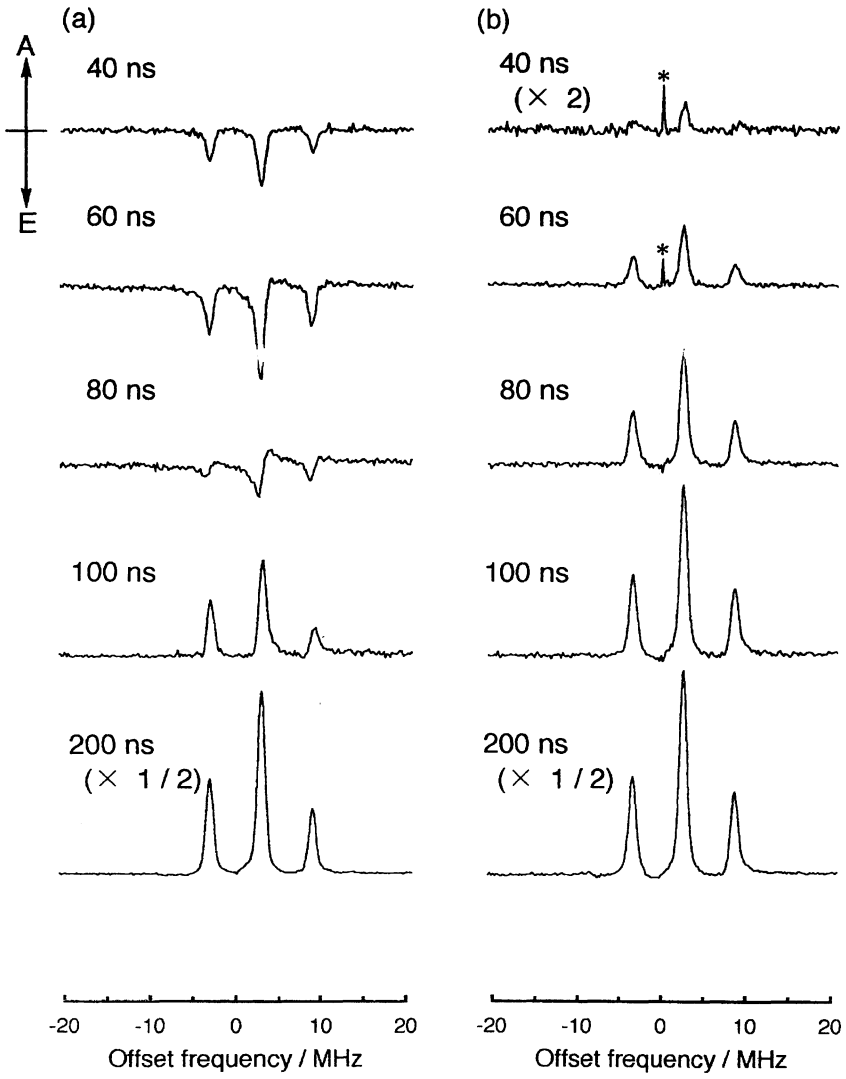

Fig. 1. Echo FT-EPR spectra obtained from the photosensitized reduction of 2,5-di-t-butyl-1,4-benzoquinone with eosin Y (a) and erythrosine B (b). The numbers inserted represent the delay time between the laser and first microwave pulses. * The artificial offset signal.

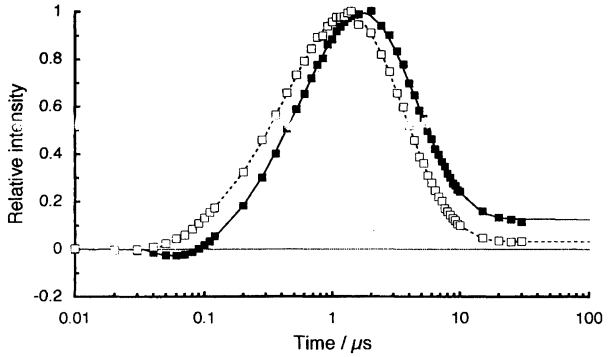

Fig. 2. Time profiles for the central line of the quinone anion radical obtained from the photolysis of 2, 5-di-*t*-butyl-1,4-benzoquinone with eosin Y (■) and erythrosine B (□) as the sensitizer. The solid and broken lines are nonlinear least squares fitting to the data points based on Eq. 1.

of the sensitizer ($^3T_1$) and the radical ($^2T_1$), as well as the time constant of the buildup of the A polarization (k^{-1}), are significantly different from each other, we can use the sum of the exponential functions for curve fitting the CIDEP intensity.[16] Thus, the time profile of the signal intensity ($S(t)$) was represented by

$$S(t) = S_E(t) + S_A(t) + S_R(t), \quad (1)$$

$$S_E(t)=A_1\left[-\exp\left\{-\left(\frac{1}{^3T_1}+k\right)(t-\Delta t)\right\}+\exp\left\{-\frac{(t-\Delta t)}{^2T_1}\right\}\right], \quad (2)$$

$$S_A(t) = A_2\left[-\exp\{-k(t-\Delta t)\}+\exp\left\{-\frac{(t-\Delta t)}{^2T_1}\right\}\right], \quad (3)$$

$$S_R(t) = A_3\left[1-\exp\left\{-\frac{(t-\Delta t)}{^2T_1}\right\}\right]. \quad (4)$$

Here, $S_E(t)$, $S_A(t)$, and $S_R(t)$ represent the growth and decay of the signals due to the emissive(E)-TM and unusual A-polarizations, as well as the thermal population, respectively. To obtain good curve fitting, the induction period (Δt) is taken into account in these equations. Based on nonlinear least-square curve fitting,[17] the growth and decay curves of the polarized signals were analyzed (Fig. 2).

The time constants (k^{-1}) of the buildup of the obtained net absorptive signals were 780 ns and 630 ns for the EY–*t*Bu$_2$BQ and ER–*t*Bu$_2$BQ systems, respectively. Assuming a pseudo-first-order reaction, $k = k_{et}[Q]$, the rate constants for the electron transfer reaction (k_{et}) were obtained as 1.3×10^9 and 1.6×10^9 mol^{-1} dm^3 s^{-1} for the EY–*t*Bu$_2$BQ and ER–*t*Bu$_2$BQ systems, respectively. These values are nearly identical to the diffusion-controlled rate constant in a 1-propanol solution. The data obtained from the analysis are summarized in Table 1. A significant heavy atom effect was observed on the enhancement factor: $f=7$ for EY–*t*Bu$_2$BQ and 29 for ER–*t*Bu$_2$BQ, respectively. The factor is defined by $f=(I_{max}-I_0)/I_0$, where I_{max} and I_0 are the maximum- and thermal-populated EPR intensities, respectively. The net absorptive spin polarization is attributable to the SOC interaction in the triplet contact RP, because the heavy atom effect works over a short-distance range.[1]

Table 1. Fitting Parameters Used for the Analysis of the Time Profiles of 2,5-Di-*t*-butylbenzoquinone Anion Radical Signals and the Enhancement Factors (f) in 1-Propanol at Room Temperature

System	$^3T_1$/ns	k_{et}/mol^{-1} dm^3 s^{-1}	$^2T_1$/μs	f
EY–*t*Bu$_2$BQ	25	1.3×10^9	3.6	7
ER–*t*Bu$_2$BQ	—	1.6×10^9	3.0	29

It is known that ST_+ mixing[18] and the radical-triplet pair mechanism (RTPM)[19—24] induce hyperfine-independent spin polarization. When the radicals have a large hfs constant, or the solvent has high viscosity, ST_+ mixing is operative. If the exchange interaction in the RP is positive, a net A-polarization should be induced by the ST_+ mixing. However, in the present systems, the hfs constant of *t*Bu$_2$BQ$^-$ is small and the viscosity of 1-propanol (2.20 cP at 20 °C) is moderate. The RTPM should generate a net emissive polarization from the triplet precursor of EY^{2-}. In addition, these mechanisms cannot explain the heavy atom effect on the observed enhancement factor.

Induction periods of Δt=30 and 60 ns were obtained for the EY–*t*Bu$_2$BQ and ER–*t*Bu$_2$BQ systems, respectively. In contrast, the Δt term is not necessary to analyze the time profile of *t*Bu$_2$BQH$^\bullet$ generated from the photooxidation of *t*Bu$_2$BQH$_2$, as is shown later. Since the CIDEP spectra can be interpreted by a normal RPM, the induction period observed in the present photoreduction systems seems to reflect the lifetime of the contact RP, which has a large exchange interaction. It is well known that many triplet exciplexes or contact RPs have a lifetime longer than 50 ns.[25—28] In the present system, the hydrogen bonding of 1-propanol as well as the Coulomb interaction between the Xn$^{-\bullet}$·2Na$^+$ and Q$^{-\bullet}$ would contribute the relatively long lifetime of the contact RP.

The reaction process for the photosensitized reduction of quinone (Q) by xanthene dye (Xn^{2-}) is depicted in Scheme 1. Here, k_q and k_{esc} are the quenching rate of the T_1 state of xanthene dye by *t*Bu$_2$BQ and the escape rate of radicals from the solvent cage; k_{ISC} and k_{isc} are the ISC rates for the contact RP and geminate RP, respectively. It can be considered that the electron spin polarization is produced by sublevel selective ISC from the triplet contact RP to the ground state by the SOC interaction.

The nonradiative rate constant for ISC is proportional to the square of the matrix element of the SOC Hamiltonian between the initial and vibrationally excited states of equal energy,

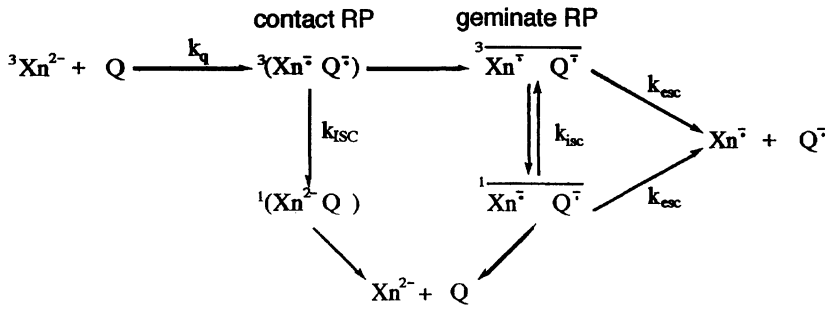

Scheme 1.

$$k_{ISC} \propto |\langle {}^3(Xn^{-\cdot}Q^{-\cdot})|H_{SO}|{}^1(Xn^{2-}Q)\rangle|^2. \quad (5)$$

$$H_{SO} = \frac{e^2}{2mc^2}\sum_i\sum_k \frac{Z^4}{r_{ik}^3}\boldsymbol{l}_i\cdot\boldsymbol{s}_i, \quad (6)$$

The SOC Hamiltonian (H_{SO}) can be described as a doubled sum over the interactions of all electrons (i) with all nuclei (k) in a first approximation in which two electron terms are neglected, where Z is the atomic number of the kth nucleus, and $\boldsymbol{l}_i$ and $\boldsymbol{s}_i$ are orbital angular and spin operators. Since the SOC interaction causes a simultaneous change in the orbital angular and spin operators, the sublevel selective back electron transfer occurs from the triplet contact

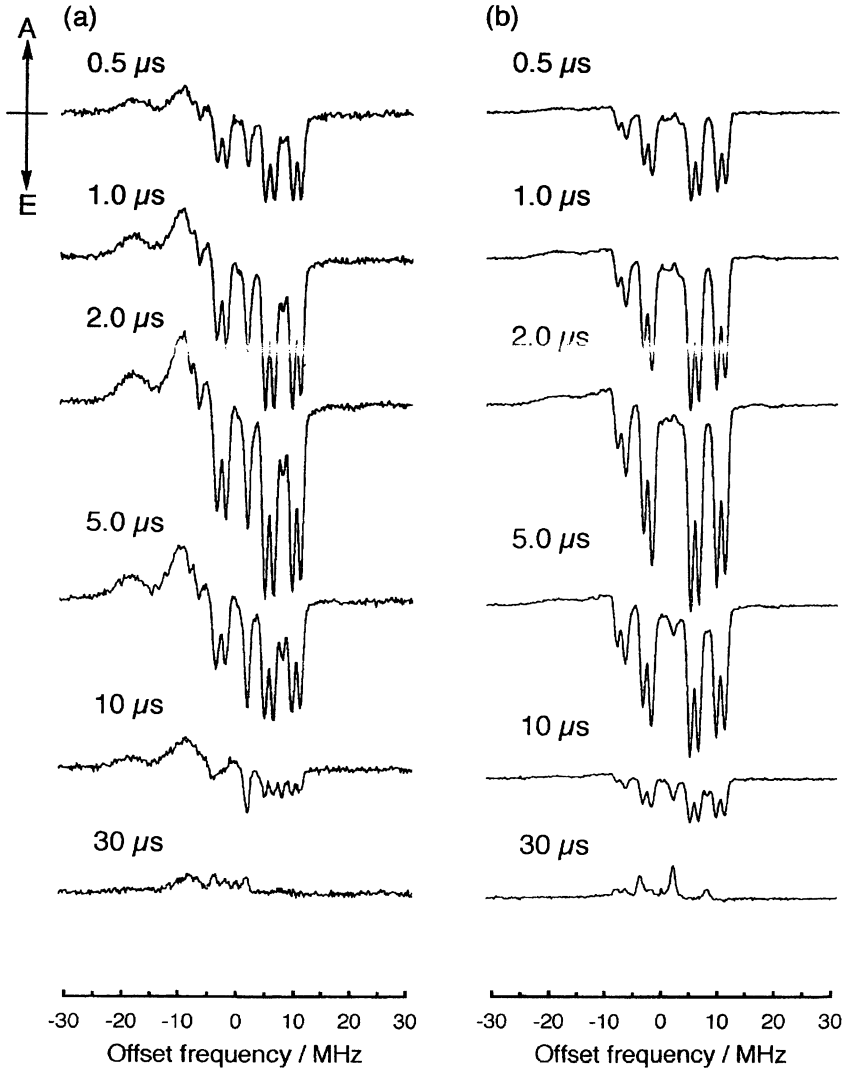

Fig. 3. Echo FT-EPR spectra observed from the photosensitized oxidation of 2,5-di-*t*-butylhydroquinone with eosin Y (a) and erythrosine (b). The numbers inserted represent the delay time between the laser and first microwave pulses.

RP to the ground state. Thus, a nonequilibrium spin population may be induced in the intermediate. The net spin polarization observed suggests that the SOC interaction enhances the ISC rate from the upper sublevel(s) of the triplet contact RP.

It can be considered from an analogy of the theory for the normal TM[29] that the enhancement factor (f) depends on the zero-field parameter (D) and the reaction rates of the sublevels (k_i),

$$f \propto |D|K, \tag{7}$$

where K is the sublevel selectivity of the back electron transfer, $K=(k_x+k_y)/2-k_z$ (x, y, and z: molecular frame coordinate axes). Since the $|D|$ value is smaller in the contact RP than in the usual T_1 states, the maximum f value might be smaller than that of the normal TM. Hayashi and Nagakura reported a $|D|$ value of 0.023 cm^{-1} for the charge-transfer triplet state of the durene–tetracyanobezene complex.[30] The f value increases along with an increase in the selectivity of the sublevel back electron transfer reactions (k_i) induced by the heavy atoms. For the normal TM, theory predicts f values up to 250; values of 10—80 were observed.[29] Therefore, the f value of 28, obtained in the present CIDEP experiment for the ER–tBu$_2$BQ system, indicates that the preferential selectivity in the triplet sublevels is induced for the back electron transfer reaction by the heavy atoms of the dyes. The solvent viscosity and polarity severely affect the f value. A detailed study is in progress.

Figure 3 depicts the echo FT-EPR spectra obtained from the photooxidation of tBu$_2$BQH$_2$ with EY and ER in 1-propanol at room temperature. Rather complicated spectra were measured and the buildup rates were relatively slow. The radicals observed in the EY–tBu$_2$BQH$_2$ system were the neutral semiquinone radical (tBu$_2$BQH$^{\bullet}$; a^{H}(1H)=0.47, a^{H}(1H)=0.17, a^{H}(1H)=0.049 mT, g=2.0043),[13] the quinone anion radical (tBu$_2$BQ$^{-\bullet}$) and the reduced form of eosin Y (EYH$^{2-\bullet}$ or EYH$_2^{-\bullet}$; a^{H}(2H)=0.335, a^{H}(3H)=0.061, a^{H}(1H)=0.029 mT, g=2.0025).[14,31] The E-TM and unusual A-CIDEP were not observed in these systems. These spectra can be interpreted by the normal radical pair mechanism (RPM), that is ST_0 mixing and the Δg effect. In the ER–tBu$_2$BQH$_2$ system, the signals due to tBu$_2$BQ$^{-\bullet}$ are very weak compared with that of the eosin Y sensitized reaction. The present results indicate that the equilibrium between tBu$_2$BQ$^{-\bullet}$ and tBu$_2$BQH$^{\bullet}$ depends on the sensitizer.

The time-profiles observed are shown in Fig. 4. Because only the normal RPM contributes to these spectra, they can be described by the sum of the growth and decay of RPM ($S_{\mathrm{RP}}(t)$) and the growth of the thermal population ($S_{\mathrm{R}}(t)$) as follows;

$$S(t) = S_{\mathrm{RP}}(t) + S_{\mathrm{R}}(t), \tag{8}$$

$$S_{\mathrm{RP}}(t) = A_1\left[-\exp\{-kt\} + \exp\left\{-\frac{t}{2T_1}\right\}\right], \tag{9}$$

$$S_{\mathrm{R}}(t) = A_2\left[1-\exp\left\{-\frac{t}{2T_1}\right\}\right]. \tag{10}$$

The time constants for buildup rates (k^{-1}) of

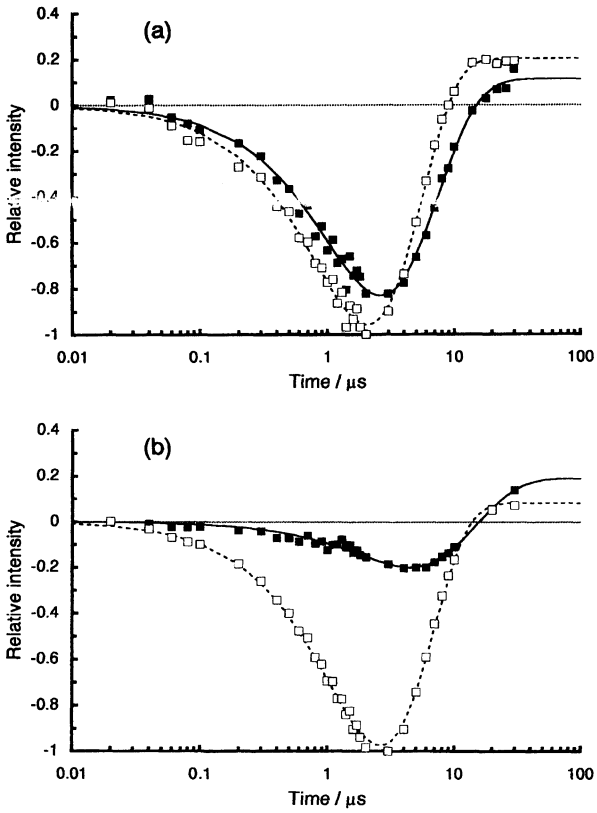

Fig. 4. Time profiles for the spectral line of the anion radical (■) and neutral semiquinone radical (□) of 2,5-di-butylbenzoquinone generated from the photooxidation of 2,5-di-t-butylhydroquinone with eosin Y (a) and erythrosine B (b). The solid and broken lines are nonlinear least squares fitting to the data points based on Eq. 8.

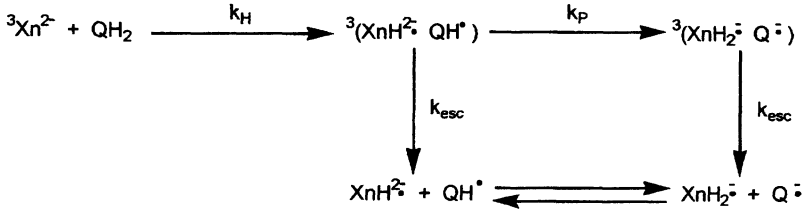

Scheme 2.

Table 2. Fitting Parameters for CIDEP Signals of Neutral 2,5-Di-*t*-butylsemiquinone Radical Generated by the Photooxidation with Eosin Y (EY) and Erythrosine B (ER) in 1-Propanol at Room Temperature

System	k_H/mol^{-1} dm^3 s^{-1}	$^2T_1$/μs
EY–*t*Bu$_2$BQH$_2$	1.5×10^8	2.3
ER–*t*Bu$_2$BQH$_2$	1.3×10^8	2.8

2.2 and 2.6 μs were obtained for *t*Bu$_2$BQH$^\bullet$ in the EY–*t*Bu$_2$BQH$_2$ and ER–*t*Bu$_2$BQH$_2$ systems, respectively. It should be noteworthy that no induction period is required for these analyses. A schematic diagram is presented for the reaction process in Scheme 2, where k_H is the rate constant for hydrogen abstraction. Based on the slow buildup rate of polarization, the hydrogen abstraction process would be a reaction-controlled one.

We can assume a pseudo first-order reaction for the hydrogen abstraction process, $k = k_H[Q]$, under the present condition. Thus, rates of $k_H = 1.5\times10^8$ mol^{-1} dm^3 s^{-1} and 1.3×10^8 mol^{-1} dm^3 s^{-1} were obtained in the EY–*t*Bu$_2$BQH$_2$ and ER–*t*Bu$_2$BQH$_2$ systems, respectively. These values are close to that reported for the oxidation of hydroquinone by rose bengal in methanol (2.5×10^8 mol^{-1} dm^3 s^{-1}).[32] The obtained data are listed in Table 2.

The buildup rate of *t*Bu$_2$BQ$^{-\bullet}$ was nearly identical to that of *t*Bu$_2$BQH$^\bullet$ in the EY–*t*Bu$_2$BQH$_2$ system. In the ER–*t*Bu$_2$BQH$_2$ system, on the other hand, the polarization increased very slowly (3.5 μs), and the intensity was very weak. It seems that the free pair also contributes to the creation of polarization.

The present results showed that the electron spin polarized EPR spectra give information about the RP intermediates as well as the spin dynamics of free radicals. In the photosensitized reduction of the present quinone by xanthene dyes, an unusual net A polarization due to the SOC-induced electron spin polarization mechanism was measured. On the other hand, normal RPM (ST_0 mixing) is operative in the photosensitized oxidation of the present hydroquinone by xanthene dyes. The results suggest the contribution of the different RP intermediates, that is, the contact RP in the former photoreduction system and solvent-separated RP in the latter photooxidation system, respectively. It is also shown that the pulsed EPR technique having a time resolution of 10 ns is quite useful for determining the reaction rate constants.

The present research was supported in part by a Grant-in-Aid on Priority-Area-Research Photoreaction Dynamics No. 06239103 from the Ministry of Education, Science and Culture.

References

1) A. Katsuki, K. Akiyama, Y. Ikegami, and S. Tero-Kubota, *J. Am. Chem. Soc.*, **116**, 12065 (1994).
2) L. Salem and C. Rowland, *Angew. Chem., Int. Ed. Engl.*, **11**, 92 (1972).
3) S. S. Shaik and N. D. Epiotis, *J. Am. Chem. Soc.*, **102**, 122 (1980).
4) C. Doubleday, N. J. Turro, and J.-F. Wang, *Acc. Chem. Res.*, **22**, 199 (1989).
5) W. Adam, L. Frohlich, W. M. Nau, and J. Wirtz, *J. Am. Chem. Soc.*, **115**, 9824 (1993).
6) U. E. Steiner and T. Ulrich, *Chem. Rev.*, **89**, 51 (1989).
7) U. E. Steiner and W. Haas, *J. Phys. Chem.*, **95**, 1880 (1991).
8) I. V. Khudyakov, Y. A. Serebrennikov, and N. J. Turro, *Chem. Rev.*, **93**, 537 (1993).
9) E. S. Klimtchuk, G. Irinyi, I. V. Khudyakov, L. A. Margulis, and V. A. Kuzmin, *J. Chem. Soc., Faraday Trans. 1*, **85**, 4119 (1989).
10) K. Kikuchi, M. Hoshi, T. Niwa, Y. Takahashi, and T. Miyashi, *J. Phys. Chem.*, **95**, 38 (1991).
11) M. Hoshi, K. Kikuchi, and H. Kokubun, *J. Photochem. Photobiol. A: Chem.*, **41**, 53 (1987).
12) M. Koizumi, S. Kato, N. Mataga, T. Matsuura, and Y. Usui, "Photosensitized Reaction," Kagakudojin, Tokyo (1978).
13) J. A. Pedersen, "Handbook of EPR Spectra from Quinones and Quinols," CRC Press, Inc., Boca Raton, Florida (1985).
14) A. Katsuki, S. Tero-Kubota, and Y. Ikegami, *Chem. Phys. Lett.*, **209**, 258 (1993).
15) G. Kroll, M. Plschau, K.-P. Dinse, and H. van Willigen, *J. Chem. Phys.*, **93**, 8709 (1990).
16) M. Ebersole, P. R. Levstein, and H. van Willigen, *J. Phys. Chem.*, **96**, 9310 (1992).
17) T. Nakagawa and Y. Oyanagi, Program system SALS for nonlinear least squares fitting in experimental sciences in "Recent Developments in Statistical Inference and Data Analysis," ed by K. Matsusita, North Holland, Amsterdam (1980), pp. 221—225.
18) F. J. Adrian *Rev. Chem. Intermed.*, **3**, 3 (1979).
19) T. Imamura, O. Onitsuka, and K. Obi, *J. Phys. Chem.*, **90**, 6741 (1986).
20) A. Kawai and K. Obi, *J. Phys. Chem.*, **96**, 52 (1992).
21) C. Blattler, F. Jent, and H. Paul, *Chem. Phys. Lett.*, **166**, 375 (1990).
22) G.-H. Goudsmit, H. Paul, and A. I. Shushin, *J. Phys. Chem.*, **97**, 13243 (1993).
23) W. S. Jenks and N. J. Turro, *J. Am. Chem. Soc.*, **112**, 9009 (1990).
24) E. N. Step, A. L. Buchachenko, and N. J. Turro, *J. Am. Chem. Soc.*, **116**, 5462 (1994).
25) M. V. Encinas and J. C. Scaiano, *J. Am. Chem. Soc.*, **101**, 7740 (1979).
26) H. Kobashi, T. Kondo, and M. Funahashi, *Bull. Chem. Soc. Jpn.*, **59**, 2347 (1986).
27) P. P. Levin and V. A. Kuzmin, *Russ. Chem. Rev.*, (*Engl. Transl.*), **56**, 307 (1987).
28) L. J. Johnston, J. C. Scaiano, and T. Wilson, *J. Am. Chem. Soc.*, **109**, 1291 (1987).
29) K. H. McLauchlan, "Modern Pulsed and Continuous-Wave Electron Spin Resonance," ed by L. Kevan and M. K. Bowman, John Wiley & Sons, New York (1990), p. 305.

30) H. Hayashi and S. Nagakura, *Mol. Phys.*, **13**, 489 (1967).
31) I. H. Leaver, *Aust. J. Chem.*, **24**, 753 (1971).
32) K. Gollnick, *Adv. Photochem.*, **6**, 1 (1968).